

1 **Subseasonal prediction of impactful California winter weather in a**
2 **hybrid dynamical-statistical framework**

3
4 Kristen Guirguis¹, Alexander Gershunov¹, Benjamin J. Hatchett², Michael J. DeFlorio¹,
5 Aneesh C. Subramanian³, Rachel Clemesha¹, Luca Delle Monache¹, and F. Martin Ralph¹

6
7 ¹*Scripps Institution of Oceanography, University of California San Diego, La Jolla, California*

8 ²*Desert Research Institute, Reno, NV*

9 ³*University of Colorado Boulder, Boulder, Colorado*

10
11 Corresponding Author: Kristen Guirguis, CW3E, Scripps Institution of Oceanography, University
12 of California, San Diego, 9500 Gilman Drive, La Jolla, CA 92093, Mail Code: 0224,
13 kguirguis@ucsd.edu.
14

15 **Key points**

- 16 • A hybrid dynamical-statistical model is developed for 1-4-week forecasts of high impact
17 California winter weather using weather regimes.
- 18 • This hybrid framework reduces the number of forecasts available, but the ones issued can
19 be interpreted with higher confidence.
- 20 • Skillful subseasonal forecasts extending lead time by 1-4 weeks could improve early
21 warnings and outcomes during extreme weather events.

22
23 **Abstract**

24 Atmospheric rivers (ARs) and Santa Ana winds (SAWs) are impactful weather events for
25 California communities. Emergency planning efforts and resource management would benefit
26 from extending lead times of skillful prediction for these and other types of extreme weather
27 patterns. Here we describe a methodology for subseasonal prediction of extreme winter weather
28 in California, including ARs, SAWs and temperature extremes. The hybrid approach combines

29 dynamical model and historical information to forecast probabilities of impactful weather
30 outcomes at weeks 1-4 lead. This methodology (i) uses dynamical model information considered
31 most reliable, i.e., planetary/synoptic-scale atmospheric circulation, (ii) filters for dynamical
32 model error/uncertainty at longer lead times, and (iii) increases the sample of likely outcomes by
33 utilizing the full historical record instead of a more limited suite of dynamical forecast model
34 ensemble members. We demonstrate skill above climatology at subseasonal timescales,
35 highlighting potential for use in water, health, land, and fire management decision support.

36

37 **Plain Text Summary**

38 California winter weather can alternate between very wet conditions from atmospheric rivers
39 making landfall along the Pacific coast to hot, dry, and windy conditions brought by Santa Ana
40 winds blowing in from the Southwest interior. Atmospheric rivers are important for water
41 resources while also causing flooding, whereas Santa Ana winds are often associated with wildfire,
42 especially following prolonged dry periods. Preparing for these types of weather events is
43 important for managing resources and protecting life and property, yet reliable forecasts beyond
44 about 7-10 days remain a challenge. We have developed a new prediction system that combines
45 information about approaching atmospheric weather patterns from weather forecast models along
46 with historical information relating those patterns to impacts over California to predict the
47 likelihood of impactful weather at 1-4 weeks lead time. By extending the window of opportunity
48 to take action, this new approach should aid in resource and emergency planning in water, land,
49 and fire sectors as well as protecting residents through improved warning systems.

50

51 **1. Introduction**

52 Extremes of California’s winter weather variability sway between heavy multiday
53 precipitation from Pacific storms associated with atmospheric rivers (ARs) and dry offshore
54 downslope winds blowing from the elevated continental interior. Drought-busting ARs cause most
55 of the region’s floods (Ralph et al. 2006, 2011, Dettinger 2013, Corringham et al. 2019) while
56 downslope winds are often associated with coastal heat waves as well as wildfire and smoke
57 impacts (Hughes and Hall 2010; Abatzoglou et al. 2013; Guzman-Morales et al. 2016; Aguilera et
58 al. 2021, Gershunov et al. 2021, Cayan et al. 2022). Winter heat waves and dry spells accelerate
59 mountain snowmelt (Hatchett et al. 2023), exacerbate drought and, particularly at the densely
60 populated coast, endanger human health (Schwartz et al. 2020, Gershunov et al. 2021). Improved
61 prediction of these types of impactful weather events is of great importance for emergency
62 preparedness and planning to mitigate impacts to society (DeFlorio et al. 2021). Climate change
63 is increasing the likelihood and intensity of extreme weather in California (e.g., Gershunov et al.
64 2019, 2021, Corringham et al. 2022, Huang and Swain 2022, Michaelis et al. 2022), highlighting
65 the need for improved forecasts across a range of lead times to aid planning and ameliorate
66 outcomes (e.g., DeFlorio et al. 2021; Oakley et al. 2023).

67 ARs are low-tropospheric jets of water vapor that produce up to 50% of California’s annual
68 precipitation (Dettinger et al. 2011, Gershunov et al. 2017). They can be beneficial and hazardous
69 (Ralph et al. 2019); replenishing water supplies, while also causing the most damaging California
70 floods (Corringham et al. 2019, Guirguis et al. 2020, 2021). Santa Ana winds (SAWs) — the
71 downslope winds of Southern California — are characterized by strong, dry, gusty northeasterly-
72 easterly winds that warm by adiabatic compression as they flow over and through the Transverse
73 and Peninsular Ranges down to sea level. SAWs can bring hot or cold temperatures, but the hot
74 variety are associated with Southern California’s wildfires (Gershunov et al. 2021, Guirguis et al.

75 2022). These hot SAWs are increasing in frequency over the historical record raising concerns
76 about future wildfire risk.

77 Numerical weather prediction has made notable advancements in recent years. Multi-
78 ensemble probabilistic forecasts provide improvements over deterministic forecasts because they
79 account for uncertainty arising from observational error, model limitations, and the chaotic nature
80 of the earth-atmosphere system (Baurer et al. 2015, Palmer et al. 2017). This improvement, along
81 with computational and satellite advances, has led to encouraging progress towards extending
82 forecast skill and lead time. However, the time limit of predictability for high-impact weather
83 events remains limited to about 1-2 weeks (Bauer et al. 2015) and warnings of heat waves or fire
84 weather are typically issued on the order of a week or less.

85 Skillful prediction of large-scale weather patterns and regime transitions has been
86 demonstrated at leads of a month or longer (Baurer et al. 2015; Gibson et al. 2020; Robertson et
87 al. 2020). This has motivated work to extend forecast lead time by focusing on atmospheric
88 circulation patterns and then inferring associated impacts for a region; leading to new operational
89 forecast products (e.g., Ferranti et al. 2015, DeFlorio et al. 2021). These studies show dynamical
90 models do have some skill at longer lead times in forecasting certain large-scale circulation
91 features, but this skill is not consistent from forecast to forecast. Progress could be made by
92 developing ways of recognizing when a subseasonal forecast is likely to be skillful or less reliable.
93 In absence of dynamical model skill, a forecast could be supplemented or replaced by a statistical
94 forecast. Here, we describe and evaluate a dynamical- statistical hybrid prediction system that uses
95 dynamical model forecasts to predict four key modes of atmospheric variability on subseasonal
96 timescales (1-4 weeks lead), filters for uncertainty and error, and then draws on known

97 relationships between these modes and high-impact West Coast weather to predict the likelihood
98 of impactful weather events.

99 Winter weather variability in California is largely modulated by four modes of atmospheric
100 variability over the North Pacific Ocean (called the “NP4 modes”, Guirguis et al. 2018, 2020a,
101 2022), named as the Baja-Pacific (BP), Alaskan-Pacific (AP), Canadian-Pacific (CP) and
102 Offshore-California (OC) modes (Figure 1a). They collectively explain most of the variance (up
103 to 89% in some locations) in mid-tropospheric circulation over a vast region over the North Pacific
104 Ocean and West Coast (Figure S1). Daily interactions between these modes result in reoccurring
105 weather patterns (Figure S2) responsible for much of California’s daily weather variability and
106 extremes, including wildfires, heat waves, and damaging floods (Figure S3, Guirguis et al. 2022a,
107 hereinafter GGR’22). These modes are also influential for California precipitation on seasonal
108 timescales due to their tendency to persist in one phase or another during a season (Guirguis et al.
109 2020a, hereinafter GGR’20).

110 Our forecast system uses the circulation regime methodology of GGR’20 and GGR’22
111 applied to 20 years of multi-ensemble hindcasts from the European Center for Medium-Range
112 Weather Forecasts (ECMWF) model as well as real-time forecasts from water year 2022
113 (WY2022). We then apply a statistical model that relates these circulation regime-based forecasts
114 to extreme weather over California. Using this dynamical-statistical hybrid approach, we
115 demonstrate skillful probabilistic forecasts of ARs, SAWs, and hot/cold temperature extremes in
116 California at subseasonal (1-4 week) lead times. By filtering out uncertain forecast periods, we
117 improve the accuracy and reliability of the forecasts relative to dynamical model skill without
118 filtering. In this novel approach, we use dynamical model information when it is likely to be
119 reliable, attempt to filter error and uncertainty, and then combine the filtered dynamical model

120 information with a statistical model to forecast an impactful weather event. At shorter lead times
121 (~1 week) the forecast is largely determined by the dynamical model information, whereas at
122 longer lead times (when the dynamical model skill degrades) the statistical information becomes
123 more important. The aim of this work is to provide tools and information for decision support to
124 improve outcomes from extreme weather events.

125

126 **2. Data**

127 *2.1. Time period of study*

128 The focus of this study is extended winter (November-February) spanning 2001-2022.

129

130 *2.2. Four Key Modes of Atmospheric Variability over the North Pacific Ocean (NP4 modes)*

131 Daily amplitudes of the NP4 modes are from Guirguis et al. (2020b, hereinafter GGR'20b), which
132 was extended through WY2022. These circulation regimes are represented using daily 500 mb
133 geopotential height (Z500) anomalies from NCEP/NCAR 2.5° Global Reanalysis (R1, Kalnay et
134 al. 1996). Anomalies were calculated by fitting and removing annual and semiannual cycles using
135 least-squares regression (Guirguis et al. 2018).

136

137 *2.3. Atmospheric Rivers (ARs)*

138 ARs landfalling the West Coast are identified using the SIO-R1 catalog of Gershunov et al. (2017),
139 available 1948-present. The methodology uses vertically integrated horizontal vapor transport
140 (IVT) and integrated water vapor (I WV) to identify elongated plumes (>1500 m) of concentrated
141 moisture (IVT>250 kg m⁻¹s⁻¹ and IWV>15mm). AR landfalls are identified when a coastal location
142 is within the AR footprint for at least one 6-hourly timestep in a day.

143

144 2.4. *Santa Ana Winds (SAWs)*

145 Santa Ana winds are identified using the daily Santa Ana Winds Regional Index (SAWRI,
146 Guzman-Morales et al. 2016). This record uses hourly surface winds spanning 65 years (1948-
147 2012) from dynamically downscaled R1 using the California Regional Spectral Model (CaRD10,
148 Kanamitsu and Kanamaru, 2007) and statistically thereafter (Guzman Morales and Gershunov
149 2019). The methodology identifies SAWs impacting coastal Southern California when
150 northeasterly wind speeds exceed local 75th percentiles.

151

152 2.5. *Precipitation and Daily Maximum Temperature*

153 Precipitation and daily maximum temperatures (tmax) are from Gridmet (Abatzaglou 2013),
154 available 1979-present at ~4km spatial resolution. Daytime hot (cold) temperature extremes are
155 defined as temperatures above (below) the historical 90th (10th) percentile after removing the
156 seasonal cycle. We focus on three regions: the Central Sierra Nevada (1) for their importance for
157 snow accumulation and water resources, as well as coastal Southern California (2) and the San
158 Francisco Bay area (3) where millions of people are exposed to hazards (Figure S4).

159

160 2.6. *ECMWF Ensemble Hindcasts*

161 We use global hindcasts of Z500 from the S2S Project database (Vitart et al. 2017) for 2001-2020.
162 We selected one model, the ECMWF model, a state-of-the-art dynamical weather forecast model
163 shown to outperform other models (e.g., Gibson et al. 2020, DeFlorio et al. 2019). Ocean coupling
164 is included in these hindcasts, but sea ice coupling is not. Data were produced with the Integrated
165 Forecast System (IFS). Hindcasts are made twice weekly yielding 34 forecasts per year over the

166 20-year period (680total), including one control and 10 perturbed ensemble members for lead
167 times out to 46-days. We focus on days 1-30 for this study.

168

169 2.7. *ECMWF Realtime Forecasts WY2022*

170 We use real-time forecasts of Z500 from the ECMWF during WY2022, produced twice weekly
171 using fifty perturbed ensemble members.

172

173 **3. Description of the Dynamical-Statistical Hybrid Model**

174 The methodology (Figure 2) uses the best available information about evolving
175 atmospheric circulation from the ECMWF, filters for error and uncertainty, and applies a statistical
176 model to predict the likelihood of an impactful weather event for a region of interest.

177

178 *3.1. Dynamical Model Input*

179 The dynamical model input consists of ECMWF forecasts of Z500 fields over a domain
180 spanning 20°S-80°N and 120-250°E for each ensemble member and lead time (Figure 2, step 1).

181

182 *3.2. Post Processing*

183 Anomaly maps are created by removing the seasonal cycle at each grid point (Section 2.2).
184 These anomaly maps are projected onto each of the four NP4 mode EOFs (e.g., GGR'20) to
185 calculate the forecast amplitude of the BP, AP, CP, and OC modes for each ensemble member and
186 lead time (Figure 2, step 2). These amplitudes provide information about the forecasted strength
187 and position of ridges and troughs over the North Pacific and along the West Coast (c.f. Figure
188 1a). There is generally strong agreement among ensemble members about the phase of the NP4

189 modes at short lead times (on the order of 7-10 days), but uncertainty can become prominent at
190 longer lead times (e.g., see growing dispersion in mode amplitudes shown in Figure 2, step_2).

191

192 3.3. *Consensus Filtering*

193 We filter for error and uncertainty using a consensus threshold of 70% (Figure 2, step 3).

194 That is, if 70% of ensemble members agree about the phase of a given mode, then we assume this
195 information is reliable. If this criterion is not met, then we consider the mode phase to be uncertain.

196 The choice of 70% is based on exploratory analysis demonstrating that a lower threshold (50-60%)

197 leads to lower skill (Figure S5a) and a higher threshold (80%) is too rarely met in weeks 3-4 (Figure

198 S5b). In Figure 2, step 3, the green and yellow shading indicates where the 70% consensus criterion

199 is met for each mode, with the remaining forecasts classified as uncertain. In physical terms, this

200 means at least 70% of ensemble members agree that a ridge or trough will persist or develop over

201 a certain location at a certain lead time. In this example, the Alaska-Pacific mode is forecast to

202 become negative around day 7 and then persist in that phase for over two weeks. The negative

203 phase of this mode is associated with a ridge over the Gulf of Alaska (c.f. Figure 1a). Knowledge

204 about a developing persistent ridge over the Alaskan Gulf is useful information for West Coast

205 weather prediction (Gibson et al. 2020, GGR'20). This forecast also indicates long-lead confidence

206 about the Baja-Pacific mode transitioning into the negative phase, and the Offshore-California

207 mode remaining negative into week 3. The model is less confident about the phase of the

208 Canadian-Pacific mode beyond day 12.

209

210 3.4. *Input to the Statistical Model*

211 The filtered dynamical model information is used as input into the statistical model. For a
212 given forecast and lead time, each of the BP, AP, CP, and OC modes can be positive, negative, or
213 unknown (Figure 2, step 4). We track the error in these dynamical NP4 phase forecasts (seen as a
214 red “x” for the CP mode in days 23-24) for the skill assessment. In this example, most of the
215 remaining forecast information (after filtering) is correct, albeit with much uncertainty at longer
216 lead times.

217

218 3.5. Statistical Model

219 A conditional probability model is used to predict the probability of a weather impact, X,
220 over different regions of the West Coast. Specifically, the model is represented as

221

$$222 \quad P(X|BP, AP, CP, OC) = \frac{P(X, BP, AP, CP, OC)}{P(BP, AP, CP, OC)} \quad Eqn (1)$$

223

224 Where P(X) is the historical conditional probability of X, and BP, AP, CP, and OC represent the
225 phase of the four NP4 modes as forecast by the dynamical model, which (from Section 3.4) can be
226 positive, negative, or unknown. The weather impact X can be any weather outcome that is driven
227 by atmospheric circulation in this region. To determine P(X), we use the NP4 dataset of GGR’20b
228 to identify days in the historical record when the same mode phase combination occurred, and then
229 compile observed outcomes on those days to quantify the historical probability of different weather
230 impacts for different locations. The statistical model will vary in complexity for each forecast and
231 lead time. Some forecasts will have 4 modes available as predictors while other forecasts will only
232 use 3, 2, or 1 mode due to uncertainty in the remaining modes. Additional detail is provided in the
233 supplement (Text S1, Figure S6). We focus on predicting AR landfalls at different West Coast

234 latitudes (32.5-55°N), SAWs in Southern California, and hot/cold temperature extremes over the
235 Sierra Nevada, Coastal Southern California, and the San Francisco Bay area.

236

237 *3.6. Hindcast Skill Assessment Methodology*

238 For the hindcast skill assessment, we bin the probabilistic forecasts $P(X)$ into three
239 categories: “low probability”, “above normal probability”, and “much above normal probability”,
240 where the upper/lower bounds for each category were determined relative to local climatology.
241 The definitions for the three categories are: <50% of climatology, 120-160% of climatology, and
242 >160% of climatology, respectively (Figure S7).

243 To assess skill, we compare the forecast conditional probability $P(X)$ with the observed
244 frequency for each type of event. A “low probability” forecast is considered skillful if the observed
245 frequency of extreme temperatures, SAWs, or ARs following these forecasts is low relative to
246 climatology (falls below the 10th percentile of the resampled distribution). The “above normal”
247 and “much above normal” forecasts are considered skillful if the observed frequency is higher than
248 the 90th percentile.

249

250 **4. Realtime Skill Assessment: Forecasts from WY2022**

251 Figure 1 shows real-time forecast information for WY2022. Verified ECMWF forecasts of
252 the NP4 modes after filtering are shown in Figure 1b. Probabilistic AR forecasts for different
253 regions along the coast are shown in Figure 1d, with the regions defined in Figure 1c. Here, the
254 NP4 mode phase information shown in Figure 1b is used as predictors for the AR forecasts shown
255 in Figure 1d (i.e., using equation 1 where X is an AR landfall at a coastal region).

256 As a first skill measure, we evaluate if the phases of the NP4 modes (Figure 1b) were
257 accurately predicted by the ECMWF model, and if the consensus filtering methodology was
258 effective at removing error (i.e., accuracy of the information used as input to the statistical model).
259 In Figure 1b, most of the information in weeks 1-2 is correct (red/blue shading) but at longer lead
260 times, an increasing number of forecasts are classified as uncertain (gray shading), and by week 4
261 most of the dynamical model information has been filtered due to uncertainty, although useful
262 information remains in week 4 for some modes. The information that remains after filtering is
263 overwhelmingly correct (91%) with only 9% error. Figure S8a examines what the forecasts would
264 look like if the NP4 mode phases were calculated from the ensemble mean without filtering.
265 Figure S8b shows the forecasts issued using the ensemble mean reference model, but which were
266 removed by the consensus filtering method. Of the forecasts removed by filtering (Figure S8b),
267 41% would have been incorrect. Unfortunately, 59% of accurate data was also eliminated by
268 filtering, but this is preferable over retaining many incorrect forecasts. To summarize, applying
269 uncertainty filtering in this hybrid dynamical-statistical framework decreases the number of
270 incorrect forecasts obtained by the raw dynamical model output by ~32%. Although the number
271 of forecasts issued in this hybrid framework are lower, the ones that are issued can be interpreted
272 with much higher confidence and reliability.

273 In WY2022, the dynamical model skillfully predicted important atmospheric circulation
274 features in week 3 and occasionally into week 4 (Figure 1b). The ECMWF skillfully predicted the
275 negative phase of the Alaskan-Pacific mode 3-4 weeks in advance during Dec-Feb, which in
276 physical terms is characterized by a ridge over the Gulf of Alaska (c.f. Figure 1a). In December,
277 the positive phase of the Canadian-Pacific mode was skillfully predicted at 3-4 weeks lead time,
278 which is associated with a trough over British Columbia. There was also skill in forecasting the

279 negative phase of the Offshore-California mode in week 3 during January and weeks 3-4 during
280 February, which is associated with a ridge offshore from California. This persistent ridge during
281 January-February is responsible for the extremely dry conditions that occurred in California and
282 contributed to the continuation of the drought during WY2022 (Figure S9).

283 Figure 1d shows real-time AR forecasts from WY2022 for four coastal regions shown in
284 Figure 1c. In Figure 1d, the top panels show the observed coastal AR IVT from Nov 1-Feb 28 and
285 the bottom panels show the AR landfall probability forecasts using the hybrid model. The forecasts
286 represent the observed AR landfall behavior that occurred in WY2022 very well with 3 weeks
287 lead, and with some skill seen at 4 weeks. In general, above (below) normal AR forecasts were
288 issued for days when AR landfalls occurred (did not occur). For example, the mid-winter dry spell
289 during December in British Columbia was correctly forecast, along with the wet periods that
290 preceded and followed. Also notable are wet December conditions followed by a dry January-
291 February along the US West coast, which was well represented in the forecasts for the Pacific
292 Northwest and Northern/Southern California.

293

294 **5. Hindcast Skill Assessment**

295 Figure 3 shows the skill assessment for 20 years of hindcast data for the NP4 modes (Figure
296 3a) and impactful weather events (Figures 3b-d).

297

298 *5.1 NP4 Modes*

299 The hindcast skill assessment for the NP4 modes, after filtering, is shown in Figure 3a. For
300 lead times of 1-2 weeks, the hindcasts are significantly skillful for all seasons (i.e., the full
301 distribution of seasonal forecasts lies above the 95% significance line). In week 3, most seasons

302 exhibit significant skill. In week 4 most seasons remain skillful, but this is less consistent where
303 the first quartile (Q1) often falls below the significance line, meaning that more than 25% of
304 forecasts are in error. In general, the forecasts of the NP4 modes, after filtering, show skill in
305 weeks 1-4.

306

307 5.2 *Hot and Cold Temperature Extremes*

308 Figure 3b shows hindcast skill for heat extremes. The hybrid model forecasts are
309 significantly skillful at weeks 1-3 lead for all regions and forecast categories. In general, “low
310 probability” forecasts are followed by a low frequency of extreme heat occurrence, whereas “above
311 normal” and “much above normal” forecasts are followed by a much higher frequency of
312 occurrence. These forecasts are statistically skillful at the 90% level.

313 There is evidence of skill in predicting extreme out-of-season heat at 4 weeks lead, but the
314 skill is not as reliable (i.e., more data points fall within the 10th-90th percentiles of the resampled
315 distribution). For Coastal Southern California and San Francisco Bay, the “low probability”
316 forecasts are not skillful at 4 weeks lead, suggesting a tendency to underestimate heat wave
317 occurrence. These regions also show inconsistent skill in week 4 forecasts for the other two
318 categories. Forecasts for the Central Sierra Nevada show significant skill at 4 weeks lead for all
319 forecast categories.

320 Figure S10 shows the skill assessment for cold extremes. The forecasts for weeks 1-3 are
321 generally skillful for the three regions and forecast categories. However, skill becomes less
322 reliable in weeks 4, especially the “below normal category. In general, extreme heat appears more
323 skillfully predictable than extreme cold. A possibility is that transient cold fronts are less

324 predictable than stationary highs, however more research is needed to identify the cause of these
325 skill differences.

326

327 5.3. *Santa Ana Winds*

328 Figure 3c shows hindcast skill for Santa Ana winds over Southern California. The results
329 are similar as for heat extremes, where the outcomes for the three forecast categories are well
330 separated and significantly skillful at weeks 1-3 lead and in week 4 for some forecast categories.
331 There is a drop in skill for the “above normal category” at 3 weeks lead, where SAWs do not
332 materialize as often as forecast, as seen by many orange data points falling below the 90th percentile
333 significance line. This drop in skill is not evident for the highest probability category, suggesting
334 that higher confidence might lead to higher skill.

335

336 5.4. *Atmospheric Rivers*

337 Figure 3d shows hindcast skill for AR landfalls at different coastal latitudes. The hybrid
338 forecasts are skillful for most locations at weeks 1-3 lead. The “below normal” forecasts are
339 followed by a low frequency of AR landfalls while the “above normal” and “much above normal”
340 forecasts are followed by an elevated frequency of AR landfalls, and these results generally show
341 significant skill at weeks 1-3 lead. At week 4, the observed AR frequency corresponding to the
342 different forecast categories is generally correct with respect to climatology. However, the skill is
343 not statistically significant across latitudes, except for the “much above normal” category, which
344 shows significant skill over latitudes 35-42 °N (much of coastal California). Overall, these results
345 are encouraging for predicting AR landfalls along the coast on subseasonal timescales.

346

347 **6. Discussion**

348 We have described and evaluated a new statistical-dynamical hybrid model, which
349 produces skillful probabilistic forecasts of temperature extremes, Santa Ana winds, and landfalling
350 ARs over California at subseasonal timescales. The model is skillful in weeks 1-3 for each impact
351 and region studied. Week 4 also shows skill, though the skill is not consistent among all variables
352 and forecast categories.

353 Because we use a hybrid approach, the potential skill is not strictly limited by the dynamical
354 weather forecast, and near-future improvements are possible through continued development of
355 the statistical model. For example, signals from lower frequency climate teleconnections could be
356 incorporated at longer lead times when the dynamical model is uncertain. Impacts of climate-scale
357 teleconnections on offshore atmospheric ridges (Gibson et al. 2020a) as well as the NP4 modes
358 (GGR'20) have been identified, and such relationships could be incorporated to extend skill and
359 lead time using this hybrid approach.

360 We focused on four impact types (hot/cold temperature extremes, SAWs, and ARs).
361 However, other applications are possible including hot/cold temperature anomalies more
362 generally, conditions driving mid-winter snowmelt (Hatchett et al. 2023), high snow level storms
363 (Shulgina et al. 2023) with rain-on-snow (Heggli et al. 2022), and other decision-specific variables
364 not represented in dynamical forecasts. The offshore wind forecasts — essential ingredients for
365 Southern California's wildfires — focused on Santa Ana winds, which were amenable to this
366 analysis given the long SAW catalog of Guzman-Morales et al. (2019). Related applications could
367 include Diablo and Sundowner winds of Northern and Central California; however the seasonality
368 of these winds requires an extension of the methodology into earlier fall and later spring
369 (Abatzoglou et al. 2020). Identifying relationships between the GGR'22 weather regimes and

370 observed live/dead fuel moisture could inform development of long-lead fire hazard models and
371 advanced warning systems using this hybrid approach.

372 Predictability of extreme precipitation in a probabilistic sense could also be explored. This
373 is especially important as both extreme winter precipitation and winter wildfires become more
374 common (Gershunov et al. 2019, Cayan et al. 2022), raising the possibility of compound extreme
375 events such as short-duration high-intensity rainfall, which can cause devastating post-fire debris
376 flows (Oakley et al. 2017, 2018a) and landslides (Rengers et al. 2020, Oakley et al. 2018b), rain-
377 on-snow flooding (Haleakala et al. 2023), as well as other precipitation patterns driving mass
378 movements such as avalanches (Hatchett et al. 2017). Improving lead time to prepare for these
379 types of events and likelihood of occurrence is crucial to prevent loss of life and mitigate damage
380 to property (Oakley et al. 2023). This approach could be applied in climate change studies, where
381 changes to atmospheric circulation identified in global climate models along with thermodynamic
382 responses could be linked to future impacts (Michaelis et al. 2023; Rhoades et al. 2023). We
383 envision these results and future updates will form the basis for real-time forecast tools with
384 possible applications for early warning systems and decision support across many sectors
385 including water resources, public health, land, and fire management in a varying and changing
386 climate.

387

388 **Open Research**

389 The NP4 dataset is available at <https://doi.org/10.6075/J0154FJJ>. The Santa Ana winds regional
390 index and the SIO-R1 AR catalog are available at <https://weclima.ucsd.edu/data-products/>. The
391 temperature gridMET dataset is available at <https://www.climatologylab.org/gridmet.html>.

392 NCEP/NCAR reanalysis is available at <https://psl.noaa.gov/data/reanalysis/reanalysis.shtml>. The
393 EMWF hindcast data are available at <https://www.ecmwf.int/en/research/projects/s2s>.

394

395 **Acknowledgements**

396 This research was funded by the U.S. Department of the Interior via the Bureau of Reclamation
397 (USBR- R15AC00003) and the California Department of Water Resources (4600010378 UCOP2-
398 11). This study also contributes to the Regional Integrated Sciences and Assessments (RISA)
399 California–Nevada Climate Applications Program, the International Research Applications
400 Program of the National Oceanic and Atmospheric Administration (NA17OAR4310284), the
401 Southwest Climate Adaptation Science Center (G18AC00320), and the National Science
402 Foundation (NSF CoPe award no. 2209058).

403

404 **References:**

- 405 Abatzoglou, J. T., 2013: Development of gridded surface meteorological data for ecological
406 applications and modelling. *Int. J. Climatol.*, **33**, 121–131.
- 407 Abatzoglou, J. T., Hatchett, B. J., Fox-Hughes, P., Gershunov, A., & Nauslar, N. J. (2021). Global
408 climatology of synoptically-forced downslope winds. *International Journal of*
409 *Climatology*, **41**(1), 31– 50. <https://doi.org/10.1002/joc.6607>
- 410 Bauer, P., Thorpe, A. & Brunet, G., 2015: The quiet revolution of numerical weather prediction.
411 *Nature*. **525**, 47–55. <https://doi.org/10.1038/nature14956>
- 412 Dettinger, M. D., F. M. Ralph, T. Das, P. J. Neiman, and D. R. Cayan, 2011: Atmospheric rivers,
413 floods and the water resources of California. *Water*, **3**, 445–478

414 Cayan, D.R., L. DeHaan, A. Gershunov, J. Guzman Morales, J.E. Keeley, J Mumford and A.D.
415 Syphard, 2022: Autumn precipitation – the competition with Santa Ana winds in determining
416 fire outcomes in Southern California. *Int. J. Wildland Fire*. **31**(11), 1056–1067.
417 <https://doi.org/10.1071/WF22065>

418 Corringham, T.W., F.M. Ralph, A. Gershunov, D.R. Cayan, and C.A. Talbot, 2019: Atmospheric
419 Rivers drive flood damages in the western United States. *Sci. Adv.*, **5**, 12, eaax4631, DOI:
420 [10.1126/sciadv.aax4631](https://doi.org/10.1126/sciadv.aax4631)

421 Corringham, T.W., McCarthy, J., Shulgina, T., *et al.*, (2022): Climate change contributions to
422 future atmospheric river flood damages in the western United States. *Sci Rep*. **12**, 13747.
423 <https://doi.org/10.1038/s41598-022-15474-2>

424 Daly, C., R.P. Neilson, and D.L. Phillips, 1994: A statistical-topographic model for mapping
425 climatological precipitation over mountainous terrain. *J. of App. Meteorol.* **33**(2): 140-158.

426 DeFlorio, M. J., D.E. Waliser, B. Guan, D.A. Lavers, F.M. Ralph, and F.Vitart, 2018: Global
427 assessment of atmospheric river prediction skill, *J. Hydrometeorol.*, **19**(2), 409-426.

428 DeFlorio, M. J., Waliser, D. E., Ralph, F. M., Guan, B., Goodman, A., Gibson, P. B., et al.,
429 2019: Experimental Subseasonal-to-Seasonal (S2S) Forecasting of Atmospheric Rivers Over
430 the Western United States. *J. Geophys. Res. Atm.*, **124**, 11242– 11265.

431 DeFlorio, M. J., F. M. Ralph, D. E. Waliser, J. Jones, and M. L. Anderson. 2021: Better
432 subseasonal-to-seasonal forecasts for water management, *EOS*,
433 **102**, <https://doi.org/10.1029/2021EO159749>

434 Dettinger MD, 2013: Atmospheric Rivers as Drought Busters on the U.S. West Coast. *J*
435 *Hydrometeorol.* **14**, 1721–1732.

436 Gershunov, A., J. Guzman Morales, B. Hatchett, R. Aguilera, T. Shulgina, K. Guirguis, J.
437 Abatzoglou, D. Cayan, D. Pierce, P. Williams, I. Small, R. Clemesha, L. Schwarz, T.
438 Benmarhnia, A. Tardy, 2021: Hot and cold flavors of southern California's Santa Ana
439 winds: Their causes, trends, and links with wildfire. *Clim. Dyn.* **57**, 2233-2248.

440 Gershunov, A., T. Shulgina, F. M. Ralph, D. Lavers, and J. J. Rutz, 2017: Assessing the climate-
441 scale variability of Atmospheric Rivers affecting the west coast of North America,
442 *Geophys. Res. Lett.* **44**, 7900-7908.

443 Gershunov, A., T.M. Shulgina, R.E.S. Clemesha, K. Guirguis, D.W. Pierce, M.D. Dettinger, D.A.
444 Lavers, D.R. Cayan, S.D. Polade, J. Kalansky and F.M. Ralph, 2019: Precipitation regime
445 change in Western North America: The role of Atmospheric Rivers. *Nature Scientific*
446 *Reports*, **9**, 9944.

447 Gibson, P.B., D.E. Waliser, B. Guan, M.J. DeFlorio, F.M. Ralph, and D.L. Swain, 2020a: Ridging
448 associated with drought across the Western and Southwestern United States:
449 characteristics, trends and predictability sources. *J. Climate*, **33**, 2485-2508.

450 Gibson, P. B., Waliser, D. E., Goodman, A., DeFlorio, M. J., Delle Monache, L., & Molod, A.,
451 2020b: Subseasonal-to-seasonal hindcast skill assessment of ridging events related to
452 drought over the Western United States. *J. of Geophys. Res. Atm.*, **125**, e2020JD033655.

453 Guirguis, K., Gershunov, A., Clemesha, R. E. S., Shulgina, T., Subramanian, A. C., & Ralph, F.
454 M., 2018: Circulation drivers of atmospheric rivers at the North American West Coast.
455 *Geophys. Res. Lett.*, **45**, 12–576.

456 Guirguis, K., A. Gershunov, M.J. DeFlorio, T. Shulgina, L. Delle Monache, A.C. Subramanian,
457 T.W. Corringham, and F. M. Ralph, 2020a: Four atmospheric circulation regimes over the

458 North Pacific and their relationship to California precipitation on daily to seasonal
459 timescales. *Geophys. Res. Lett.*, **47**, e2020GL087609.

460 Guirguis, K., Gershunov, A., DeFlorio, M. J., Shulgina, T., Delle Monache, L., Subramanian, A.
461 C., et al., 2020b: Data from: Four atmospheric circulation regimes over the North Pacific
462 and their relationship to California precipitation on daily to seasonal timescales. *UC San*
463 *Diego Library Digital Collections*, <https://doi.org/10.6075/J0154FJJ>

464 Guirguis, K., Gershunov, A., Hatchett, B. et al., 2022: Winter wet–dry weather patterns driving
465 atmospheric rivers and Santa Ana winds provide evidence for increasing wildfire hazard
466 in California. *Clim. Dyn.*, **60**, 1729–1749.

467 Guzman Morales, J., A. Gershunov, J. Theiss, H. Li and D.R. Cayan, 2016: Santa Ana Winds of
468 southern California: Their climatology, extremes, and behavior spanning six and a half
469 decades. *Geophys. Res. Lett.*, **43**, 2827– 2834.

470 Guzman Morales, J. and A. Gershunov, 2019: Climate change suppresses Santa Ana Winds of
471 Southern California and sharpens their seasonality. *Geophys. Res. Lett.*, **46**, 2772– 2780.

472 Haleakala, K., W.T. Brandt, B.J. Hatchett, D. Li, D.P. Lettenmaier, and M. Gebremichael, 2022:
473 Watershed memory amplified the Oroville rain-on-snow flood of February 2017, *PNAS*
474 *Nexus*, **2**, 1-15.

475 Hatchett, B. J., S. Burak, J. J. Rutz, N. S. Oakley, E. H. Bair, and M. L. Kaplan, 2017: Avalanche
476 Fatalities during Atmospheric River Events in the Western United States. *J.*
477 *Hydrometeor.*, **18**, 1359–1374.

478 Hatchett, B. J., Koshkin, A. L., Guirguis, K., Rittger, K., Nolin, A. W., Heggli, A., et al.,
479 2023: Midwinter dry spells amplify post-fire snowpack decline. *Geophys. Res. Lett.*, **50**,
480 e2022GL101235.

481 Heggli, A., Hatchett, B., Schwartz, A., Bardsley, T., & Hand, E. (2022). Toward snowpack runoff
482 decision support. *IScience*, **25**(5), 104240. <https://doi.org/10.1016/j.isci.2022.104240>

483 Huang, X. and D. Swain, 2022: Climate change is increasing the risk of a California megaflood.,
484 *Sci. Adv.* **8**, eabq0995.

485 Hughes, M., & Hall, A., 2010: Local and synoptic mechanisms causing Southern California's
486 Santa Ana winds. *Clim. Dyn.*, **34**, 847–857.

487 Kalnay, E., et al., 1996: The NCEP/NCAR 40-year reanalysis project, *Bull. Am. Meteorol. Soc.*,
488 **77**, 437–471.

489 Kanamaru, H., & Kanamitsu, M., 2007: Fifty-Seven-Year California Reanalysis Downscaling at
490 10 km (CaRD10). Part II: Comparison with North American Regional Reanalysis, *Journal of*
491 *Climate*, **20**, 5572-5592.

492 Mariotti, A., et al., 2020: Windows of Opportunity for Skillful Forecasts Subseasonal to Seasonal
493 and Beyond. *Bull. Am. Meteorol. Soc.*, **101**, E608-E625.

494 Michaelis, A. C., Gershunov, A., Weyant, A., Fish, M. A., Shulgina, T., & Ralph, F. M.,
495 2022: Atmospheric river precipitation enhanced by climate change: A case study of the storm
496 that contributed to California's Oroville Dam crisis. *Earth's Future*, **10**, e2021EF002537.

497 Oakley, N.S., Lancaster, J.T., Kaplan, M.L., and Ralph F.M., 2017: Synoptic conditions associated
498 with cool season post-fire debris flows in the Transverse Ranges of southern California. *Nat*
499 *Hazards* **88**, 327–354.

500 Oakley, N., J. Cannon, F., Munroe, R., Lancaster J., Gomberg D., and Ralph F.M., 2018a: Brief
501 communication: Meteorological and climatological conditions associated with the 9 January
502 2018 post-fire debris flows in Montecito and Carpinteria, California, USA. *Nat. Hazards*
503 *Earth Syst. Sci.*, **18**, 3037-3043.

504 Oakley, N. S., J. T. Lancaster, B. J. Hatchett, J. Stock, F. M. Ralph, S. Roj, and S. Lukashov,
505 2018b: A 22-Year Climatology of Cool Season Hourly Precipitation Thresholds Conducive
506 to Shallow Landslides in California. *Earth Interact.*, **22**, 1–35.

507 Oakley, N. S., and Coauthors, 2023: Toward probabilistic post-fire debris-flow hazard decision
508 support. *Bull. Amer. Meteor. Soc.*, <https://doi.org/10.1175/BAMS-D-22-0188.1>, in press.

509 Palmer, T., 2017: The primacy of doubt: Evolution of numerical weather prediction from
510 determinism to probability, *J. Adv. Model. Earth Syst.*, **9**, 730–734.

511 Rengers, F.K., McGuire, L.A., Oakley, N.S. *et al.*, 2020: Landslides after wildfire: initiation,
512 magnitude, and mobility. *Landslides* **17**, 2631–2641.

513 Rhoades, A.M., Zarzycki, C.M., Inda Díaz, H.A., et al., 2023: Recreating the California New
514 Year's flood event of 1997 in a regionally refined Earth system model. *ESS Open Archive*.

515 Robertson, A. W., Vigaud, N., Yuan, J., & Tippett, M. K., 2020: Toward Identifying Subseasonal
516 Forecasts of Opportunity Using North American Weather Regimes, *Monthly Weather*
517 *Review*, **148**, 1861-1875.

518 Schwarz L., B.J. Malig, J. Guzman Morales, K. Guirguis, A. Gershunov, R. Basu and T.
519 Benmarhnia, 2020: The health burden of fall, winter and spring heat waves in Southern
520 California and contribution of Santa Ana Winds. *Env. Res. Lett.* **15**, 054017.

521 Shulgina, T., Gershunov, A., Hatchett, B.J. *et al.* Observed and projected changes in snow
522 accumulation and snowline in California's snowy mountains. *Clim Dyn* (2023).
523 <https://doi.org/10.1007/s00382-023-06776-w>

524 Vitart, F., and Coauthors, 2017: The Subseasonal to Seasonal (S2S) Prediction project database.
525 *Bull. Amer. Meteor. Soc.*, **98**, 163–173.

526

527

528

529

530

531

532

533

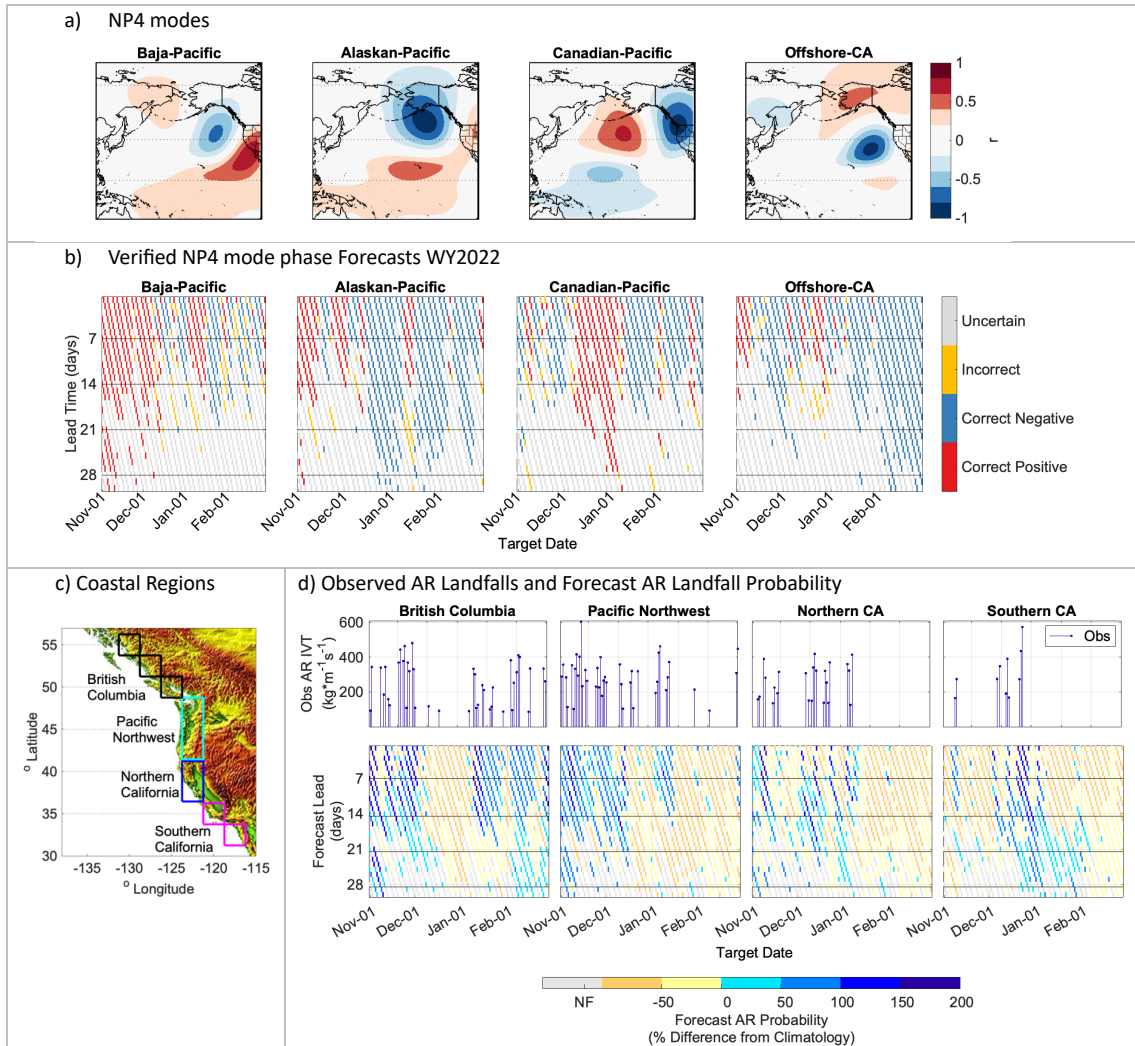
534

535

536

537

538



539

540 **Figure 1.** (a) Positive phase of the NP4 modes shown in units of correlation (r) between each mode
 541 and the raw Z500 data. (b) Validated real-time forecasts of the NP4 mode phase from WY2022,
 542 where each individual forecast is displayed on a diagonal line, the x-axis gives the target date from
 543 1Nov-28Feb, the y-axis gives the lead time from 1-30 days, red (blue) shading indicates that a
 544 mode was correctly forecast to be in the positive (negative) phase, yellow shows forecast error,
 545 gray shows when forecasts were classified as uncertain. (c) Map showing four West Coast regions.
 546 (d) Observed and forecast AR behavior during WY2022 for the four regions shown in (c), where
 547 the top four panels (blue stem plots) show regionally averaged observed daily AR IVT during
 548 WY2022, the bottom four panels show the hybrid forecasts for each region at different lead times,

549 where each forecast is shown on a diagonal line, the x-axis gives the target date, the y-axis gives
550 lead time, blue indicates above normal AR probability forecasts (wet), yellow/orange shows low
551 probability forecasts (dry), gray indicates uncertainty (no forecast, NF).

552

553

554

555

556

557

558

559

560

561

562

563

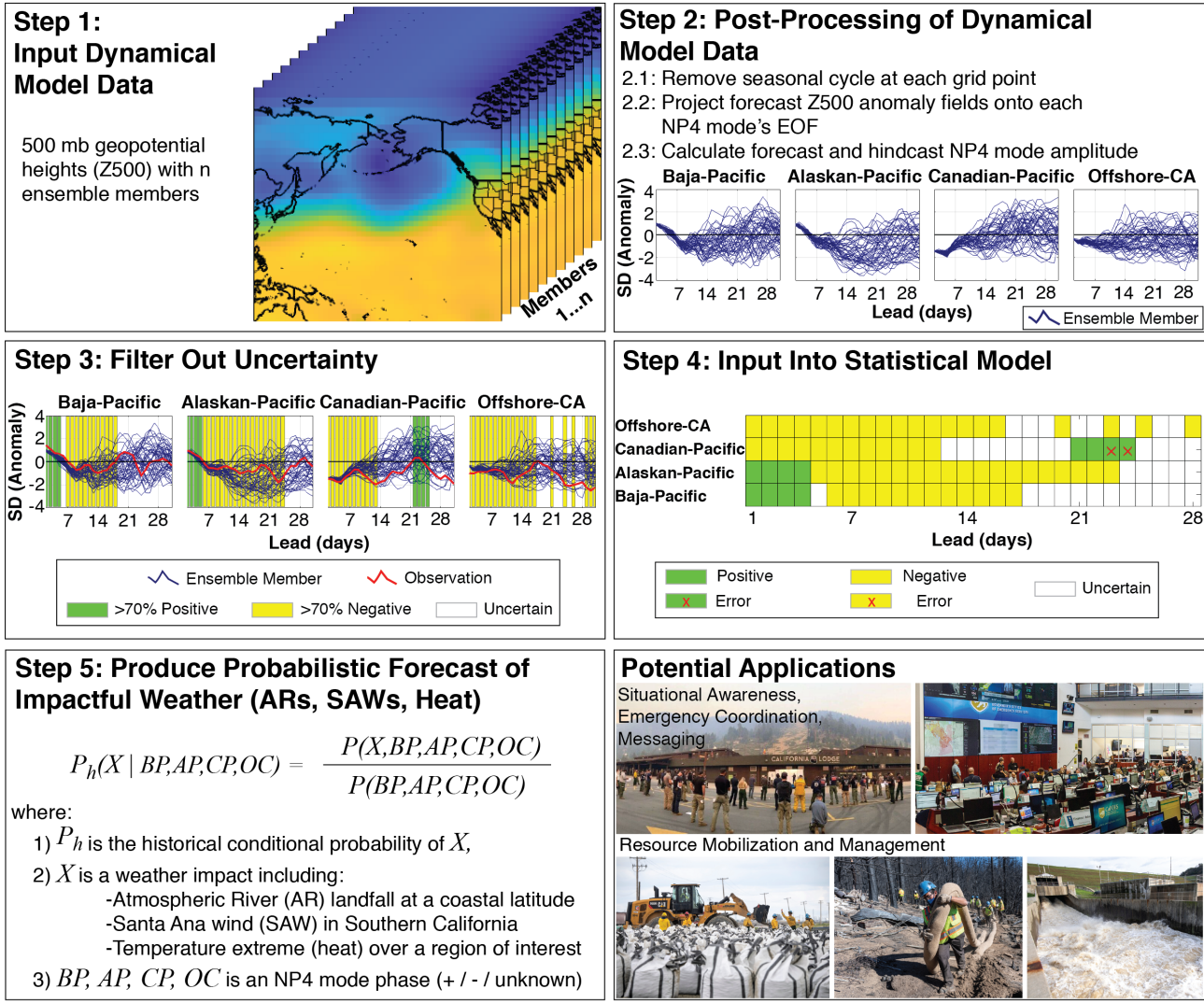
564

565

566

567

Subseasonal Hybrid Dynamical-Statistical Modeling Methodology



568 **Figure 2.** Description of the statistical-dynamical hybrid model. Step 1 describes the dynamical
 569 model input. Step 2 illustrates postprocessing, specifically the NP4 mode amplitudes (units of
 570 standard deviations) as calculated from Z500 forecasts from 50 ensemble members for 1-30 days
 571 lead. Step 3 shows consensus filtering where green (yellow) indicates >70% of ensemble members
 572 agree that the mode will be positive (negative), white indicates uncertainty, and the red line shows
 573 observations. Step 4 shows the input into the statistical model, where each mode is input as

574 positive, negative, or unknown/uncertain, and the red “x” shows error relative to observations.

575 Step 5 describes the statistical model.

576

577

578

579

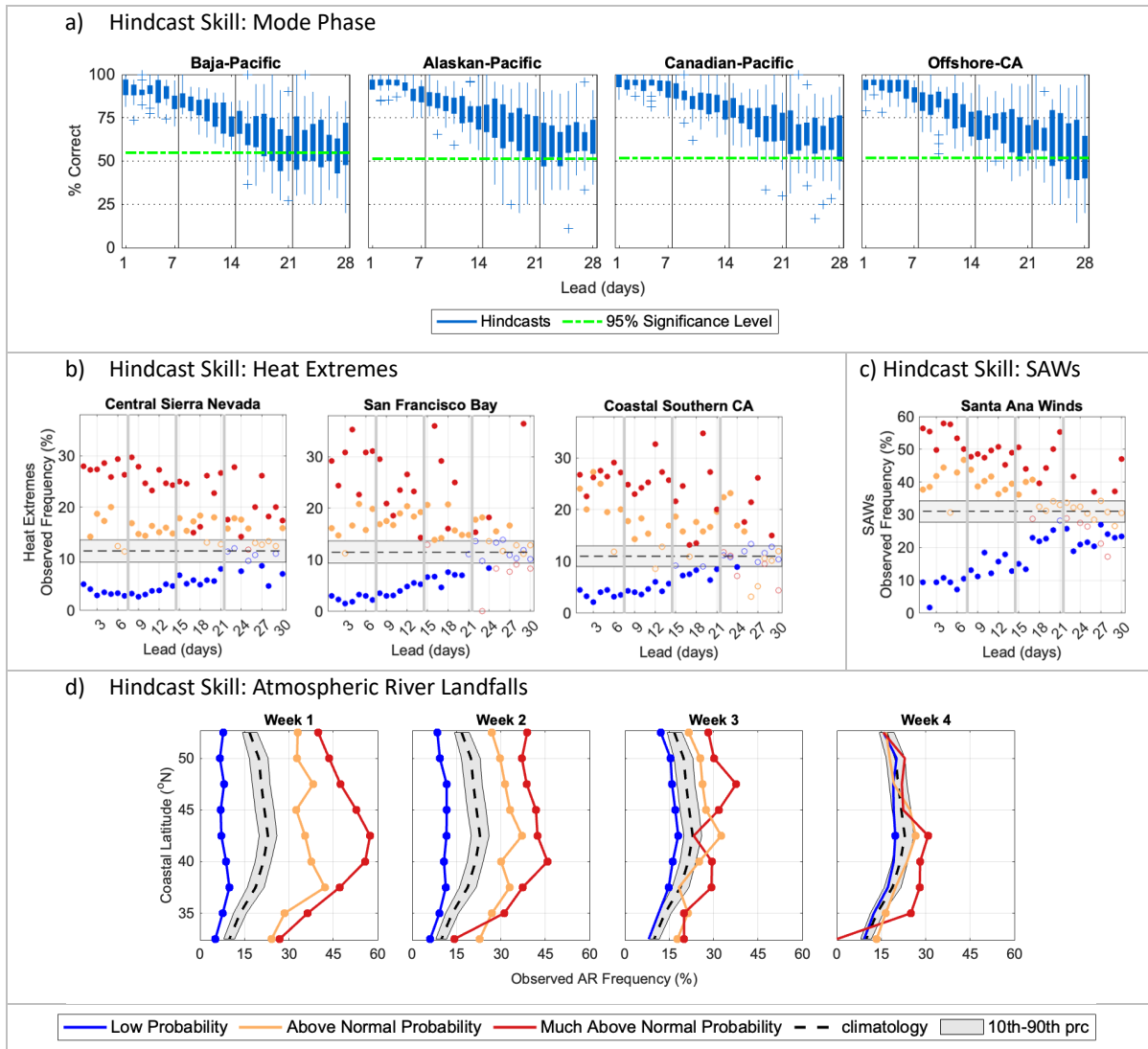
580

581

582

583

584



585

586 **Figure 3.** (a) Hindcast skill assessment of the NP4 mode phase, after filtering, where the y-axis

587 gives the percent of forecasts in a season that were correct, the x-axis shows lead time, the boxes

588 include datapoints falling within the interquartile range with lines extending to the 10th-90th

589 percentiles, and the green line shows the 95% significance level. (b-c) Hindcast skill assessment

590 of heat waves and SAWS, respectively, where the y-axis shows observed event frequency

591 following three forecast categories: low (blue), above normal (orange), and much above normal

592 (red) probability. (d) Hindcast skill assessment of AR landfalls at different coastal latitudes (y-

593 axis) shown at the weekly resolution. The gray shaded area in b-d gives the 10th-90th percentiles

594 of the resampled distribution, and the dashed black line shows climatology. Filled markers indicate
595 statistically significant skill (90% level).